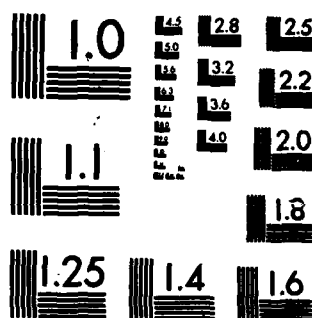MICROCOPY RESOLUTION TEST CHART
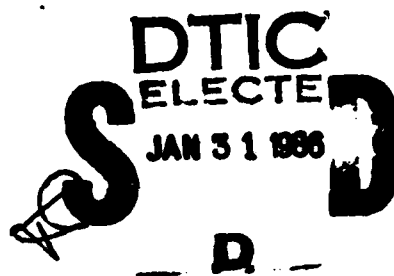
NATIONAL BUREAU OF STANDARDS-1963-A

AD-A163 529

Reverse-Wave Suppressor Mirror Effects
on CW HF Unstable Ring Laser Performance

J. M. BERNARD, R. A. CHODZKO, and H. MIRELS
Aerophysics Laboratory
Laboratory Operations
The Aerospace Corporation
El Segundo, CA 90245

30 September 1985

DTIC
ELECTE
JAN 3 1 1986

D

DTIC FILE COPY
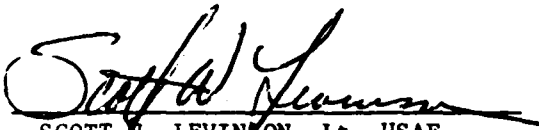
This report was submitted by The Aerospace Corporation, El Segundo, CA 90245, under Contract No. F04701-83-C-0084 with the Space Division, P.O. Box 92960, Worldway Postal Center, Los Angeles, CA 90009. It was reviewed and approved for The Aerospace Corporation by W. P. Thompson, Director, Aerophysics Laboratory.

Lt Scott W. Levinson/YNS was the Air Force project officer.

This report has been reviewed by the Public Affairs Office (PAS) and is releasable to the National Technical Information Service (NTIS). At NTIS, it will be available to the general public, including foreign nationals.

This technical report has been reviewed and is approved for publication. Publication of this report does not constitute Air Force approval of the report's findings or conclusions. It is published only for the exchange and stimulation of ideas.

SCOTT W. LEVINSON, Lt, USAF
MOIE Project Officer
SD/YNS

JOSEPH HESS, GM-15
Director, AFSTC West Coast Office
AFSTC/WCO OL-AB

SECURITY CLASSIFICATION OF THIS PAGE (When Data Entered)

REPORT DOCUMENTATION PAGE	READ INSTRUCTIONS BEFORE COMPLETING FORM

1. REPORT NUMBER	2. GOVT ACCESSION NO.	3. RECIPIENT'S CATALOG NUMBER
SD-TR-85-92	AD-A163529	

4. TITLE (and Subtitle)	5. TYPE OF REPORT & PERIOD COVERED
REVERSE-WAVE SUPPRESSOR MIRROR EFFECTS ON CW HF UNSTABLE RING LASER PERFORMANCE	
	6. PERFORMING ORG. REPORT NUMBER TR-0084A(5764)-1

7. AUTHOR(s)	8. CONTRACT OR GRANT NUMBER(s)
Jay M. Bernard, Richard A. Chodzko, and Harold Mirels	F04701-83-C-0084

9. PERFORMING ORGANIZATION NAME AND ADDRESS	10. PROGRAM ELEMENT, PROJECT, TASK AREA & WORK UNIT NUMBERS
The Aerospace Corporation El Segundo, Calif. 90245	

11. CONTROLLING OFFICE NAME AND ADDRESS	12. REPORT DATE
Space Division Los Angeles Air Force Station Los Angeles, Calif. 90009-2960	30 September 1985
	13. NUMBER OF PAGES 33

14. MONITORING AGENCY NAME & ADDRESS(If different from Controlling Office)	15. SECURITY CLASS. (of this report)
Air Force Weapons Laboratory Kirtland AFB, N.M. 87117	Unclassified
	15a. DECLASSIFICATION/DOWNGRADING SCHEDULE

16. DISTRIBUTION STATEMENT (of this Report)

Approved for public release; distribution unlimited.

17. DISTRIBUTION STATEMENT (of the abstract entered in Block 20, if different from Report)

18. SUPPLEMENTARY NOTES

19. KEY WORDS (Continue on reverse side if necessary and identify by block number)

Lasers
Reverse-wave suppression
Reverse-wave suppressor mirror
Ring resonators
Unstable resonators

20. ABSTRACT (Continue on reverse side if necessary and identify by block number)

The effect of a reverse-wave suppressor (RWS) mirror on the performance of a CW HF unstable ring laser has been measured in terms of forward/reverse-wave power ratio (P_F/P_R) and forward-wave beam quality. It was found that a well-aligned RWS mirror gave the best suppression $(P_F/P_R \simeq 100)$ and diffraction-limited beam quality. Resonator performance degraded rapidly with misalignment of the RWS mirror: a 200-μrad tilt reduced P_F/P_R to 2.5 and the beam quality by a factor of 2. The forward-wave near-field pattern —

DD FORM 1473
(FACSIMILE)

19. KEY WORDS (Continued)

20. ABSTRACT (Continued)

showed distinct fringes as the RWS mirror was misaligned, suggesting that a
higher-order mode was causing the beam quality to degrade. A novel
technique was developed to reduce the alignment sensitivity of the RWS
mirror. By use of a distorted relay mirror, an aberrated ($\cong 2\ \lambda$) reverse
wave was fed back into the ring. The aberrated reverse-wave feedback
greatly reduced the sensitivity of resonator performance to RWS mirror tilt.
Diffraction-limited beam quality and good suppression ($P_F/P_R \cong 20$) was
observed over a tilt range of 600 μrad. It is postulated that the aberrated
RWS mirror provides sufficient feedback to suppress the reverse wave over a
wide angular range, yet not enough to produce higher-order transverse modes
in the forward wave.

PREFACE

CONTENTS

FIGURES

TABLES

6

I. INTRODUCTION

Reverse-wave suppression in ring resonators has been studied by Faxvog[1,2] for stable, single-line He-Ne lasers. Suppression yielding forward-to-reverse power ratios (P_F/P_R) greater than 100 was reported and discussed theoretically. Experimental studies of single-line unstable ring lasers have been presented for both homogeneously broadened[3,4] and inhomogeneously broadened[5] gain media. Frieberg et al.[4] observed that P_F/P_R is relatively insensitive to the radius of curvature or axial location of the suppressor mirror. The above authors emphasized the dependence of the forward-to-reverse power ratio on the degree of coupling between the two waves, and when a feedback mirror was used, its coupling was optimized by careful alignment. The present study includes measurements of beam quality as well as P_F/P_R, and thus provides a performance parameter by which the misalignment sensitivity of various suppressor mirrors can be compared.

We have previously published a theoretical and experimental study[6] demonstrating that excellent reverse-wave suppression (P_F/P_R up to 92) can be obtained in a __multiline__, inhomogeneously broadened, multimode continuous-wave hydrogen fluoride (CW HF) unstable ring laser. In the present study, we have avoided the thermal distortion problem that limited CW HF laser beam quality to $1/n^2 = 0.5$ in Ref. 6, and have implemented diagnostics that simultaneously record $P_F(t)$, $P_R(t)$, and $n^2(t)$. [Here, $1/n^2$ is the ratio expressing the experimental laser's power through an aperture in the far field (of Airy disc size) divided by the power for the same laser with uniform near-field phase and intensity.] We can therefore measure the effect of various types of feedback on CW HF ring laser performance.

In particular, we first present experimental results for a well-aligned reverse-wave feedback mirror. Forward-to-reverse power ratio, beam quality, and temporal stability are noted. The effects of suppressor mirror tilt and partial feedback are then examined. Finally, the use of an aberrated relay mirror to reduce laser sensitivity to suppressor mirror tilt is examined.

7

II. EXPERIMENTAL APPARATUS

A schematic diagram of the ring resonator is shown in Fig. 1. The single-pass round-trip length of this ring is 12.5 m. Mirrors M_3 and M_4 comprise a telescope of magnification 1.72. Two double-sided output scraper mirrors, with hole diameters of 10.5 and 14.3 mm, were used in these tests. This allowed us to test at two values of equivalent Fresnel number N_{eq}. For a ring resonator,

$$N_{eq} = [a^2(M^2 - 1)]/[2\lambda(L_1 M^2 + L_2 M + L_3)]$$

where a is the scraper hole radius and λ is the laser wavelength. Referring to Fig. 1, $L_1 = 3.5$ m is the distance traveled by the forward wave from the scraper mirror to M_3, $L_3 = 8.4$ m is the distance from M_4 back to the scraper, and $L_2 = 0.6$ m is the telescope length, from M_3 to M_4. The latter mirrors have radii of curvature -1.72 m and $+2.98$ m, respectively. In the present case, $N_{eq} = 0.5$ and 0.9, respectively, for the two scrapers.

The large value of $L_1 + L_2 + L_3$, chosen to ensure that forward and reverse waves compete for the same gain, makes N_{eq} slightly less than unity for mode sizes on the order of the gain region size. The $N_{eq} = 0.5$ resonator was chosen first because the gain region uniformly fills the mode, as shown in Fig. 2. The $N_{eq} = 0.9$ case is the largest practical Fresnel number that we could test, since the gain slightly underfills the mode (see Fig. 2). Since no significant effect of Fresnel number on the performance parameters measured by us was found, we believe that our results are representative of resonators having even larger values of N_{eq}.

These resonators are used with 2 mm and 5 mm downstream decentering of the optical axis, respectively, in order to avoid obscuration of the laser mode by the nozzle exit hardware. Note that the reverse wave reflects from a relay mirror on its way to and from the suppressor mirror.

The gain generator and gain medium properties are discussed in Ref. 7. The spatial relationship between the gain distribution for $P_1(4)$ and

9

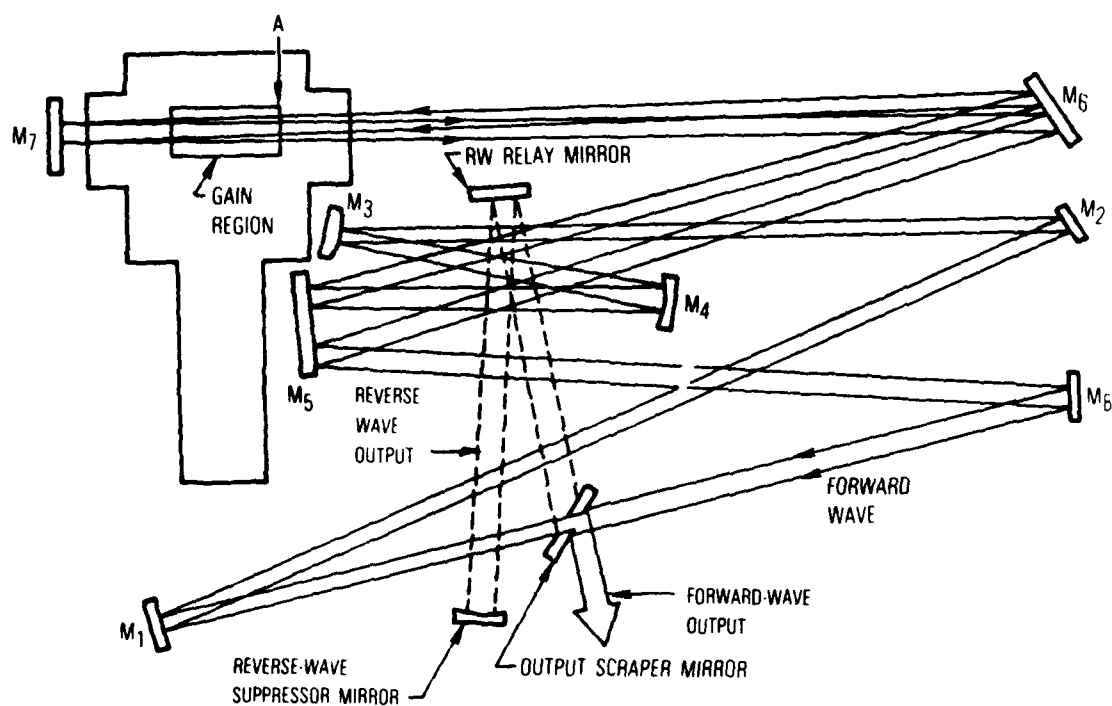Fig. 1. Optical Schematic Diagram of the Unstable Ring Resonator. Gain region flow is in the vertically upward direction.
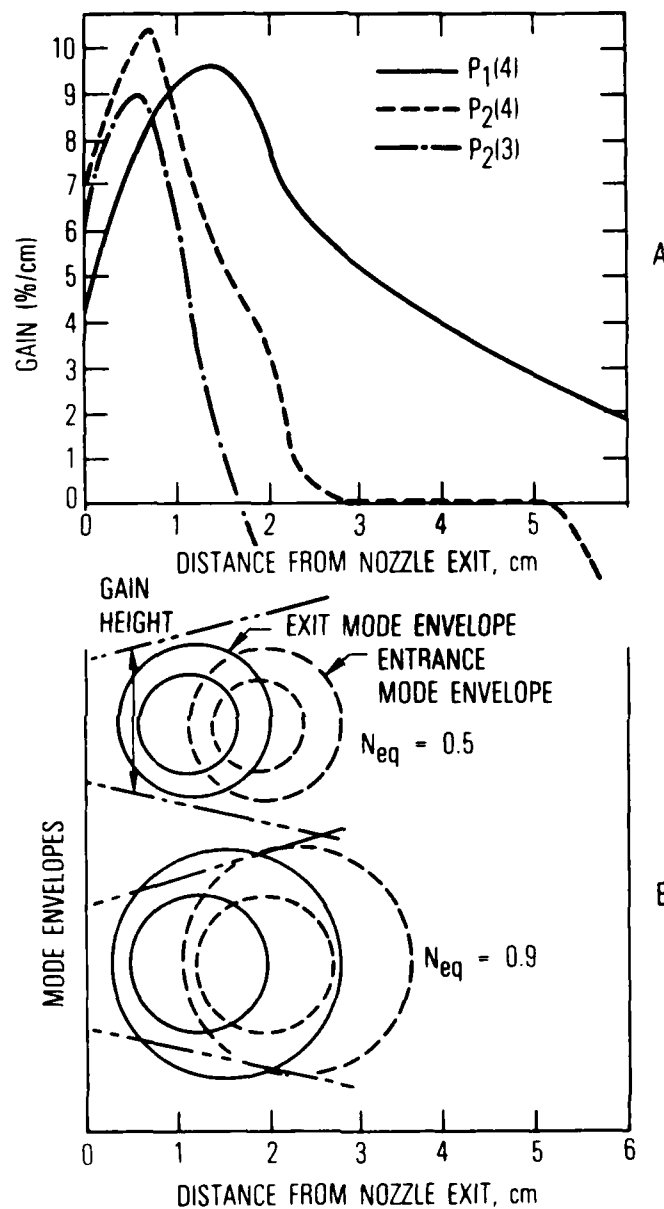
Fig. 2. (a) Gain Distribution as a Function of Downstream Distance for $P_1(4)$ and P_2(3 and 4), Compared to the Forward-Wave Mode Envelope Entering and Exiting the Gain Region (Station A in Fig. 1). (b) Forward-Wave Mode Envelopes, Showing the Variation of Gain Volume Height with Downstream Distance.

11

P_2(3 and 4) and the forward-wave mode envelope at the beginning and end of its two passes through the gain region is shown in Fig. 2 for both Fresnel numbers. In general, the P_1(J) lines fill the mode volume for both passes, while the P_2(J) lines do not. The large gain gradient within the mode volume on some lines explains our observation of a sensitivity of the laser output line spectrum to millimeter changes in the location of the optic axis within the gain region.

A schematic diagram of the diagnostic facilities used in these tests is given in Fig. 3. The forward-wave beam quality (BQ) is measured as $1/n^2$: the percentage of the far-field focused power transmitted through an aperture of diameter equal to that of the first null in the theoretical Airy pattern (based on a uniform-intensity and uniform-phase annulus in the near field) divided by the percentage of the total power theoretically contained within the first null. Good beam quality is considered to be $0.9 < 1/n^2 < 1.0$, while lower numbers denote worse BQ.

Three room-temperature indium-arsenide detectors provide the time-dependent laser intensity data for these experiments. They are illuminated by (1) a forward-wave beam that is transmitted through the aperture, (2) a forward-wave reference signal, and (3) a reverse-wave reference signal. Suitably amplified, the detector outputs provide waveforms that are stored on a digital oscilloscope. These waveforms can then be divided by each other to give the percent transmission (proportional to n^{-2}) through the aperture, and the forward-to-reverse power ratio as functions of time. These waveforms can also be analyzed to determine the rms fluctuations in the powers or BQ. Two spectrometers with detector arrays[8] were used to document the forward- and reverse-wave spectral contents. Typically, the ring laser simultaneously outputs seven spectral lines, with most of the power on P_1(4) and P_2(5 and 6). In the absence of reverse-wave suppression, the same lines appear in the forward and reverse directions, and perturbations in the forward and reverse waveforms for a given line are anticorrelated.

An intracavity shutter was used to limit the heat loading on the resonator and diagnostic mirrors. The laser on-time was limited to 30 msec,
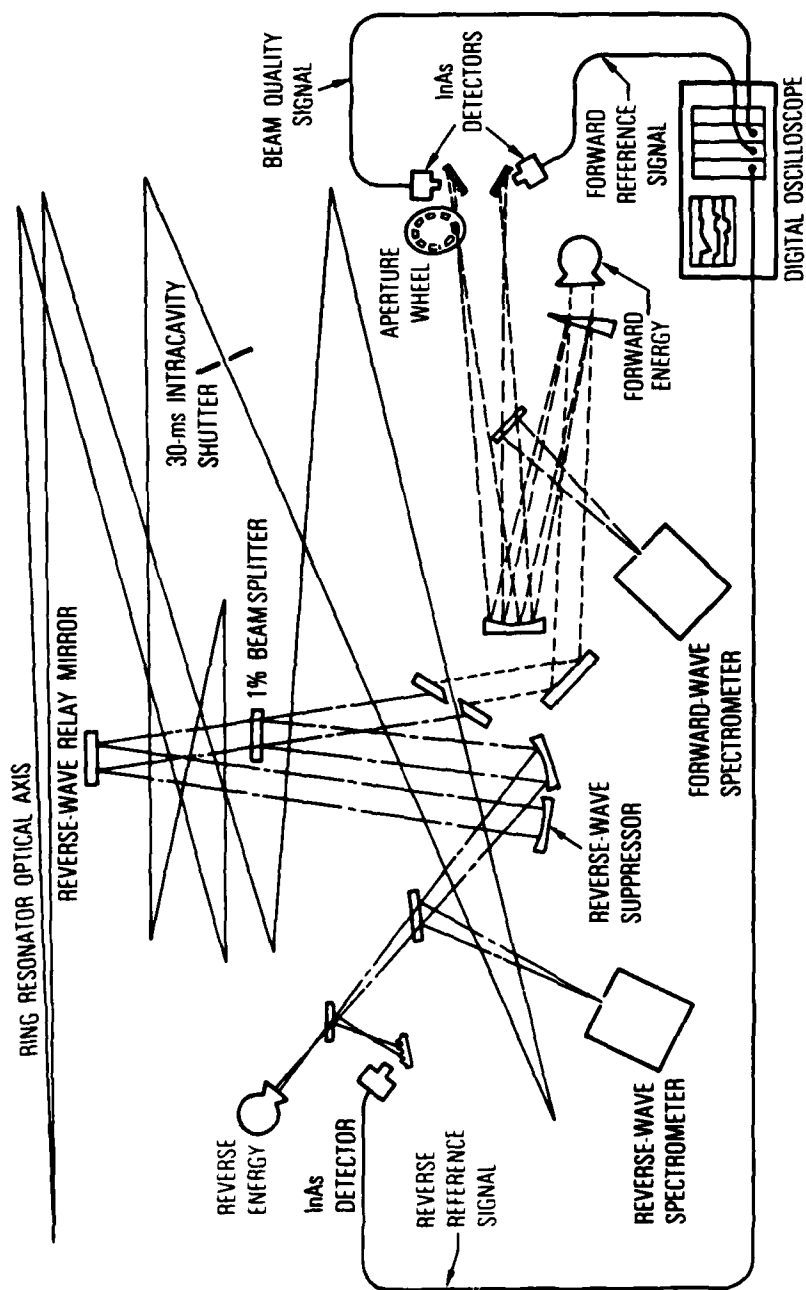
Fig. 3. Schematic of the Optical Diagnostic Facilities

13

which is comparable to the time scale that we measured for the start of beam-quality degradation due to thermal distortion. The digital oscilloscope thus records only data taken while the mirrors have their proper figure. With optimized resonator and suppressor alignment, diffraction-limited operation ($n^{-2} = 1.00$) was obtained over this time scale.

Two pyroelectric energy detectors are used, with digital readouts that display the total energy output in the forward and reverse waves during the laser on-time. These measurements provide an accurate average P_F/P_R, and calibrate their respective waveforms (as recorded on the digital oscilloscope) to yield $P_F(t)$ and $P_R(t)$.

III. EXPERIMENTAL RESULTS

The performance of the CW HF ring laser was first investigated for
the case of an aligned reverse-wave suppressor mirror and for cases with
suppressor mirror tilt. The effect of partial forward-wave feedback was then
studied. Finally, the use of an aberrated reverse-wave relay mirror, to
reduce suppressor mirror tilt sensitivity, was investigated. These results
are noted below.

A. ALIGNED REVERSE-WAVE SUPPRESSOR MIRROR

Measurements were made to characterize laser performance by using an
aligned suppressor mirror (having a spherical figure within 1/10 of the HF
laser wavelength) whose +10-m curvature matched the theoretical radius of
curvature of the reverse wave at the suppressor mirror location. The quanti-
tative performance of the N_{eq} = 0.5 and 0.9 resonators, with and without the
aligned suppressor mirror, is summarized in Table 1. Shown are the beam
quality of the forward wave, forward and reverse powers, their rms fluctuation
intensity σ, and the far-field centerline brightness parameter P_F/n^2 (which is
proportional to the forward-wave power contained within the focused spot).
Typical of the results of a given test series, these data display the improve-
ment in performance obtainable by means of a well-aligned suppressor mirror.
Not only is the forward power enhanced with no loss in beam quality, but the
fluctuation intensity σ has been halved. The ability of the suppressor mirror
to improve temporal stability is in accord with the theoretical results of
Ref. 6. The beam quality of the N_{eq} = 0.9 resonator is less than that for
N_{eq} = 0.5, as a result of partial-aperture lasing in the vertical direction
caused by the gain region being vertically smaller than the mode (see Fig. 2).

A two-step procedure was used to ensure that the suppressor mirror was
aligned. In the first step, the suppressor mirror was adjusted so that the
near-field interference fringes, in the forward wave, were axisymmetric (these
fringes, discussed in the next section, could be seen to respond to suppressor
tilt). The second step was to minimize the power in the reverse wave. When
the suppressor mirror was near alignment, we found an extreme sensitivity of

15

Table 1. Performance of the Two Ring Resonators with the Mirror Out, and with a Well-Aligned RWS Mirror In. Here, σ is the rms power fluctuation in watts.

N_{eq}	Suppressor	n^2_F	P_F, W	P_R, W	P_F/P_R	σ_F, W	σ_F/P_F	σ_R, W	σ_R/P_R	P_F/n^2, W
0.5	Out	1.0	214	67	3.2	32	0.15	44	0.66	214
	In	1.0	242	3.9	62	12	0.05	2.2	0.58	242
0.9	Out	1.1	135	115	1.2	16	0.12	25	0.22	123
	In	1.1	245	4.2	58	13	0.05	2.0	0.48	223

16

reverse-wave power to suppressor mirror tilt. Excellent suppression ($P_F/P_R = 100$) could be obtained within 10 microradians (μrad) of optimum alignment. Greater suppression ($P_F/P_R > 1000$) was occasionally achievable, with great difficulty, but was stable for only minutes. The measurements of suppression reported in Table 1 are for an average of 20 runs, and include examples of runs that were within ± 10 μrad of optimum. Systematic measurement of tilt sensitivity in the 10-μrad range requires improved room-temperature stabilization and mirror mount adjustment.

B.   EFFECT OF SUPPRESSOR MIRROR TILT

The effect of suppressor mirror tilt was evaluated by observing inter-ference patterns in the forward-wave output beam and by measuring P_F/P_R and beam quality as a function of suppressor mirror tilt. These results are dis-cussed below.

1.   INTERFERENCE PATTERNS

Typical forward-wave near- and far-field intensity patterns are noted in Fig. 4 for the cases of no suppressor mirror, an aligned suppressor mirror, and a tilted suppressor mirror. These patterns were observed on thermally sensitive paper (Thermo-fax) that darkens with the application of heat. In the case of no suppressor mirror, Fig. 4a, the near field was a nearly uniform annulus and the far field was a diffraction-limited spot ($n^2 = 1$). For the case of an aligned suppressor mirror, Fig. 4b, faint circular interference fringes were observed in the near field. The far-field spot was again symmetric and diffraction-limited. Figures 4c and 4d indicate that the effect of tilt is to drive the near-field intensity in the tilt direction, here hori-zontally upstream. High-visibility, asymmetric interference fringes are seen in the near field. With increase in tilt, the far field elongates and eventually appears as two spots. Thus, far-field beam quality degrades with tilt.

The patterns in the near field may be viewed as the interference of two (or more) phase-related forward-wave modes. One of these is the fundamental (low-loss) forward-wave mode associated with the well-aligned resonator. The second wave may be viewed as a higher-order (high-loss) forward-wave mode that

17

NEAR FIELD

REDUCED GAIN
REGION DUE TO
H₂ INJECTOR
GEOMETRY

FLOW

EXPANDED FAR FIELD

(a)

(b)

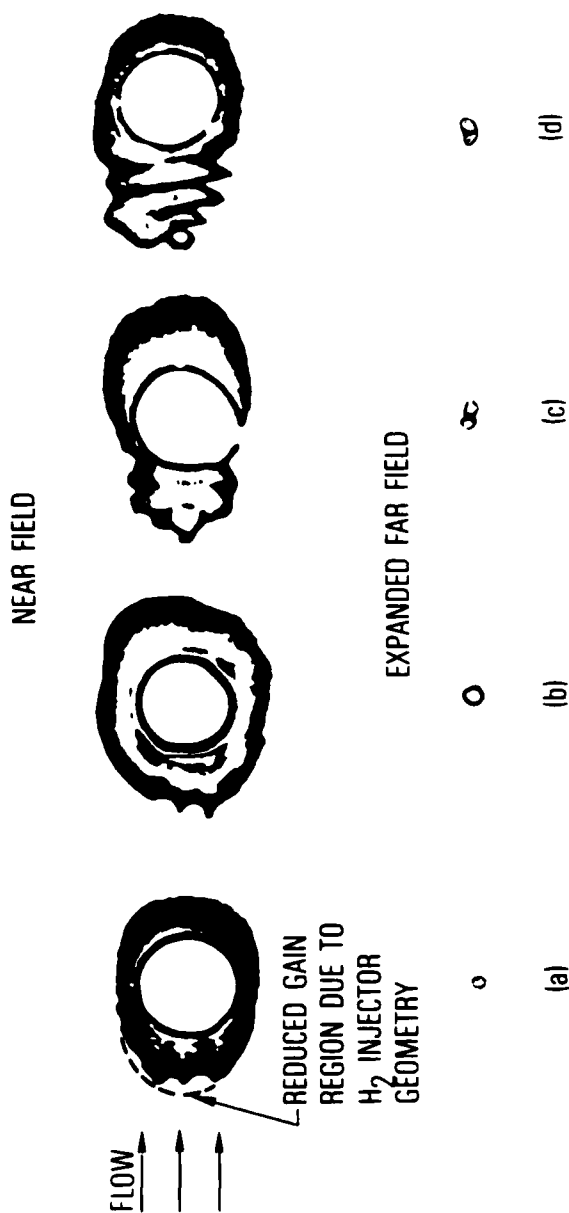(c)

(d)

Fig. 4. Qualitative Near- and Far-Field Intensity Distributions of the
Forward Wave for the N_{eq} = 0.5 Resonator. (a) Without suppression,
(b) with aligned suppressor, (c) with suppressor tilted 300 μrad,
and (d) with suppressor tilted 600 μrad. Suppressor mirror tilt is
horizontal and drives the near field in an upstream direction.
(Patterns are observed on thermal paper.)

18

is initiated and maintained by the injection of the reverse wave into the resonator by the suppressor mirror. The reinjected reverse wave also partly supports the fundamental low-loss forward wave, thereby partly suppressing the corresponding fundamental low-loss reverse wave. When the suppressor mirror is aligned, the reinjected reverse wave is weak and supports a low-loss symmetric mode similar to the fundamental forward-wave mode. Hence there is no loss in beam quality and the interference fringes are weak. With increase in tilt, the reverse-wave power is increased, leading to increased power in the higher-order modes, increased near-field fringe visibility, and poorer beam quality.

The presence of the fringes indicates that the two modes are phase-related. This is in accord with ring resonator theory, which indicates that when a suppressor mirror is used the forward and reverse waves are phase-locked during stable operation.

The present discussion represents a first attempt to explain the interference patterns associated with a tilted reverse-wave suppressor mirror. Current physical optics studies[9,10] of the coupled forward- and reverse-wave modes will lead to a more comprehensive understanding of these patterns.

2. LASER PERFORMANCE

The effect of suppressor mirror tilt on forward-to-reverse power ratio and beam quality for the $N_{eq} = 0.5$ resonator is given in Fig. 5. This figure is an average of many tests. As expected, both P_F/P_R and $1/n^2$ decrease with increasing tilt, with at most a 10-μrad tilt tolerance for optimum P_F/P_R, and a 50-μrad tilt tolerance for beam quality.

As previously noted, far-field centerline brightness is proportional to P_F/n^2. This quantity, for the data in Fig. 5, is included in Fig. 6 as the dashed line denoted "conventional relay mirror." The far-field brightness is relatively insensitive to P_F/P_R, for $P_F/P_R > O(10)$, and therefore depends primarily on beam quality. Hence the brightness curve in Fig. 6 is similar to the curve for $1/n^2$ in Fig. 5. The limit of very large suppressor mirror tilt ultimately corresponds to that for the case of no suppressor mirror. In this
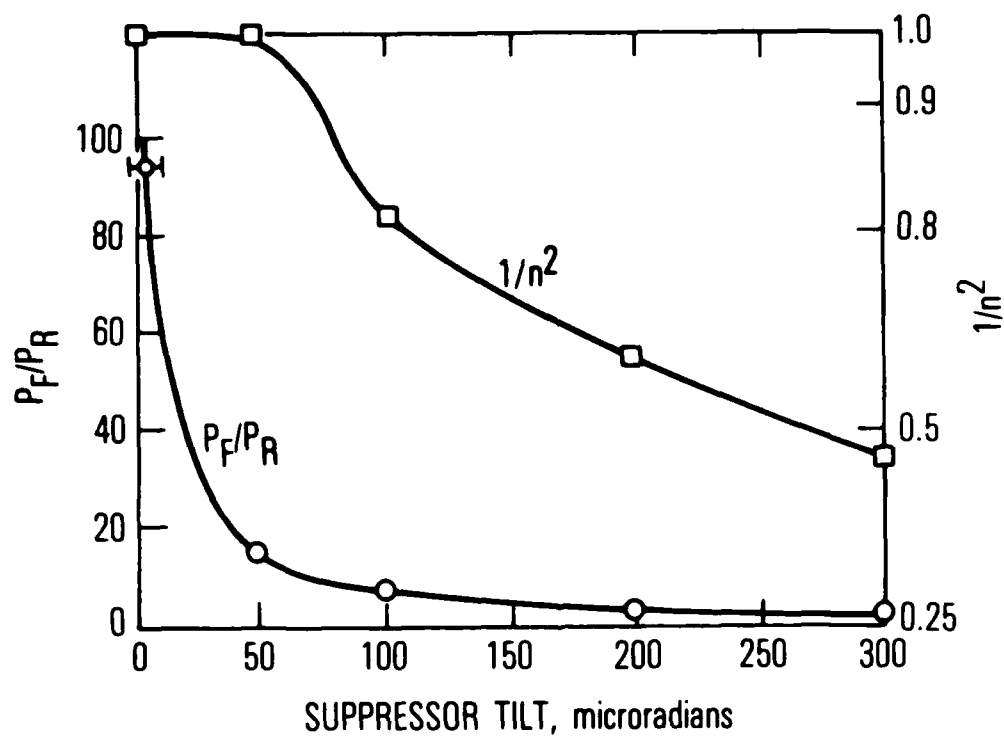
Fig. 5. Measured Dependence of the Forward-to-Reverse-Wave Power Ratio and
Beam Quality on Horizontal Tilt of the Suppressor Mirror for the
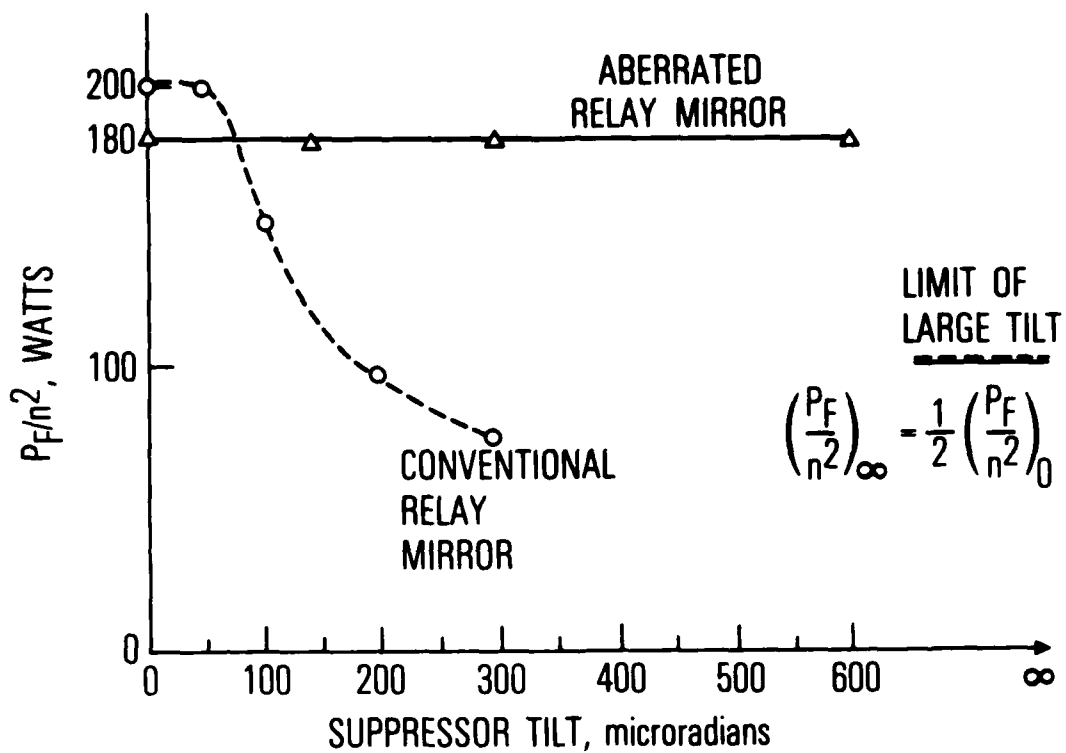$N_{eq} = 0.5$ Resonator

Fig. 6. Effect of Suppressor Mirror Tilt on Forward-Wave Far-Field
Brightness for Cases of Conventional and Aberrated Relay Mirrors for
the N_{eq} = 0.5 Resonator

limit, $P_F/P_R \to 1$, $1/n^2 \to 1$, and P_F/n^2 approaches half of the value for zero tilt, as noted in Fig. 6.

C. PARTIAL FEEDBACK

The effect of partial suppressor mirror feedback is examined analytically and experimentally in this section. We consider the case where the ring resonator length is adjusted so that the forward and reverse waves compete for the same gain medium. In this limit,[6]

$$P_F/P_R = \overline{\sqrt{R^-/R^+}} \tag{1a}$$

$$\equiv \overline{\sqrt{(R_M^- + R_b^-)/(R_M^+ + R_b^+)}} \tag{1b}$$

where R^+ denotes the net reflection coefficient for reflection of the forward wave into the reverse direction. Also, $R^+ \equiv R_M^+ + R_b^+$, where R_M^+ is the contribution of a forward-wave suppressor mirror (if present) and R_b^+ is the contribution of diffractive and surface-particle backscatter. A similar definition applies for R^-. In general, $R_b^+/R_b^- = 0(1)$.

An experiment was conducted to evaluate $R_b^\pm$ and to validate Eq. (1). The $N_{eq} = 0.9$ resonator was used. For convenience, the forward wave was suppressed and reverse-wave power and beam quality were measured. Various percentages of forward-to-reverse feedback were used. In this case, $R_M^- = 0$, $R_M^+ \neq 0$, and Eq. (1) becomes

$$P_F/P_R = \overline{\sqrt{R_b^-/R_M^+}} \left[1 + 0(R_b^+/R_M^+) \right] \tag{2}$$

A schematic diagram of this experiment is shown in Fig. 7. A flat feedback mirror provided 92% return, and two filters transmitting 50% were inserted sequentially to obtain 23% and 6% feedback of the forward wave into the reverse direction; the latter corresponds to R_M^+. These tests are

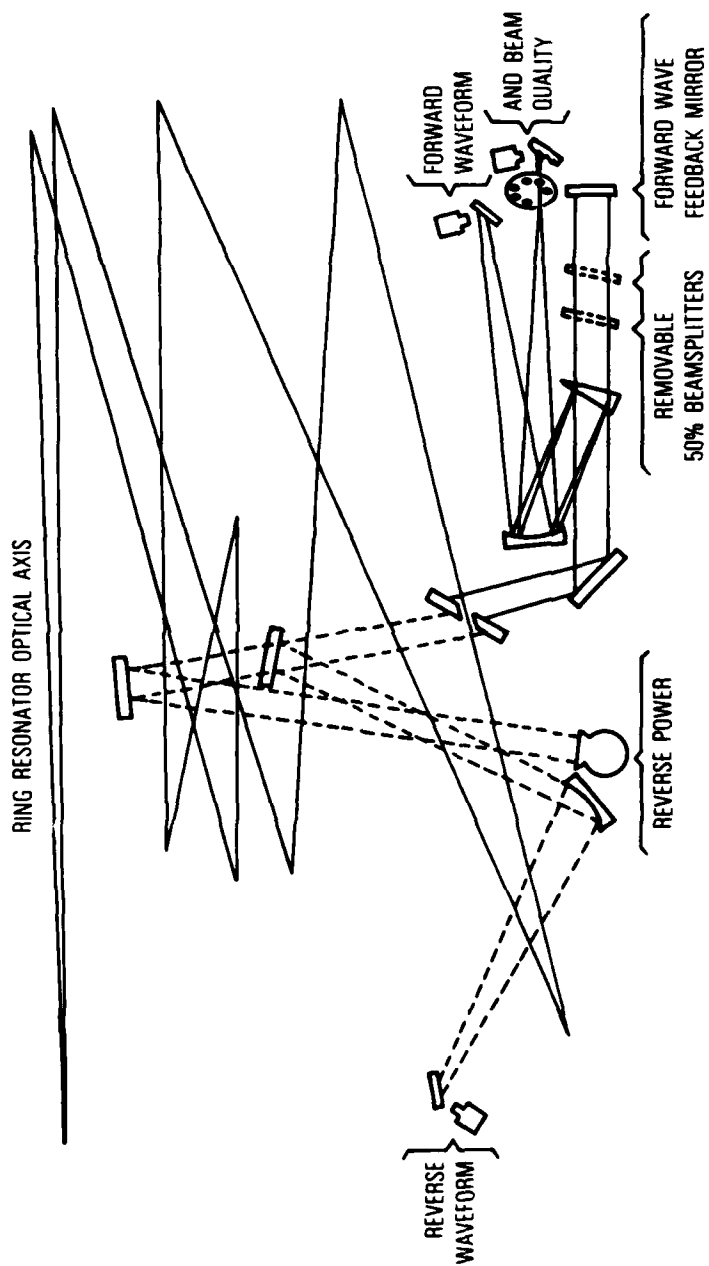22

RING RESONATOR OPTICAL AXIS

REVERSE
WAVEFORM

REVERSE POWER

REMOVABLE
50% BEAMSPLITTERS

FORWARD WAVE
FEEDBACK MIRROR

FORWARD
WAVEFORM

AND BEAM
QUALITY

Fig. 7.   Schematic Diagram of the Forward-Wave Feedback Tests

23

summarized in Table 2. Substitution of the values of P_F/P_R from this table for $R_M^+ = 0.06$, 0.23, and 0.92 into Eq. (2) yields $R_b \times 10^4 = 1.98$, 1.49, and 1.68, respectively. The approximate constancy of the values for R_b^- tends to validate Eq. (1) and thereby the theory of Ref. 6. It is seen that for the present resonator, $R_b^- = O(10^{-4})$. It may be assumed that R_b^+ is of the same order so that the approximation in Eq. (2) is valid. Finally, it is seen that, for a well-aligned suppressor mirror, only a small percentage of feedback is needed to achieve significant suppression. Thus an aligned reverse-wave suppressor mirror with $R_M^- = 0.01$ will result in $P_F/P_R = 10$, no loss in forward-wave beam quality, and a forward-wave far-field brightness within 10% of the value for $R_M^- = 1.00$. This result suggests the use of an aberrated relay mirror to reduce ring resonator performance sensitivity to tilt, as discussed in the next section.

D.   ABERRATED REVERSE-WAVE RELAY MIRROR

The extreme sensitivity of a conventional ring laser to suppressor mirror tilt, and the substantial suppression obtained by partial feedback, suggested that a suppressor mirror that spread its feedback over a wide angular range may provide suppression with reduced tilt sensitivity. This can be achieved by the use of an aberrated reverse-wave relay mirror. The effect of such a mirror on beam quality could not be predicted, but it was hoped to be minimal; if the feedback that reinforces the forward-wave fundamental mode is comparable to the feedback that tends to reinforce higher-order modes, the fundamental mode will have the lowest loss and should dominate.

An aluminum substrate was prepared as a reverse-wave relay mirror using conventional machine-shop polishing techniques, with no regard to surface figure. A photograph and an interferogram (taken with 633-nm light, at +18.5-m radius of curvature) of this mirror appear in Fig. 8. The interferogram shows that the mirror surface has random undulations of +3 microns at spatial frequencies of 5 cm^{-1} and less. The reflectance as a function of angle along several meridians (spaced by 30°) of this mirror is compared to an optical quality (less than 150 nm surface misfigure at less than 1 cm^{-1}

24

Table 2. Performance of the N_{eq} = 0.9 Resonator with Varying Percentages of Forward-Wave Feedback

% FW Fed Back	n_F^2	P_F, W	P_R, W	P_R/P_F	σ_F, W	σ_F/P_F	σ_R, W	σ_R/P_R	$\bar{R}_b \times 10^{-4}$
0	1.1	122	97	0.81	18	0.148	62	0.639	–
6	–	19	331	17.4	10	0.526	25	0.075	1.98
23	1.1	8	320	39.3	8	1.0	35	0.109	1.49
92	–	6	442	74	4.4	0.733	36	0.081	1.68

A   B

Fig. 8.   (a) Photograph and (b) Interferogram of the Aberrated Relay Mirror

26

spatial frequency) flat mirror in Fig. 9. The ordinate in this figure is the power transmitted through a fixed aperture (of Airy disc size) at the nominal reflected-wave focal point. The aberrated mirror provides a focal spot of roughly ten times the angular extent of a conventional mirror. Polishing scratches perpendicular to the 60° meridian are responsible for the large angular spread of scattered light in that direction.

The performance of the N_{eq} = 0.5 resonator was investigated by using the aberrated relay mirror in the reverse-wave feedback path. Because of relay mirror aberration, the zero-tilt alignment position of the suppressor mirror was uncertain to within ±200 µrad. A nominal zero-tilt position was chosen and the suppressor mirror tilt was systematically increased to a value of 600 µrad. The resulting variation of P_F/P_R and $1/n^2$ with tilt is given in Fig. 10 and the corresponding variation of P_F/n^2 is given in Fig. 6. Figure 10 indicates a slight deterioration in beam quality from the value n^2 = 1.0, and values of P_F/P_R in the range of 10 to 25. No systematic variation of these quantities with suppressor mirror tilt is observed. This result may be contrasted with the severe degradation of P_F/P_R and beam quality with suppressor mirror tilt noted in Fig. 5 for a conventional relay mirror. The effect of tilt on far-field brightness for the two relay mirrors is indicated in Fig. 6. The value of P_F/n^2 for the aberrated relay mirror is seen to be insensitive to suppressor mirror tilt for the entire tilt range under investigation. Moreover, P_F/n^2 is within 10% of the value for an aligned suppressor mirror with a conventional relay mirror. In the present case, the aberrated mirror provides superior far-field brightness when suppressor mirror tilt exceeds 100 µrad.

In the case of the aberrated relay mirror, the insensitivity of P_F/P_R to tilt is a consequence of the large angular spread of the feedback, as shown in Fig. 9. The insensitivity of beam quality to tilt is a result of the fact that the amount of reverse-wave power fed back into individual higher-order forward-wave resonator modes is inadequate to compensate for the higher losses in these modes compared with the fundamental. Hence the fundamental (high beam quality) mode dominates. An aberrated relay mirror is expected to be useful in cases where suppressor mirror tilt and/or figure control is difficult or costly.

27
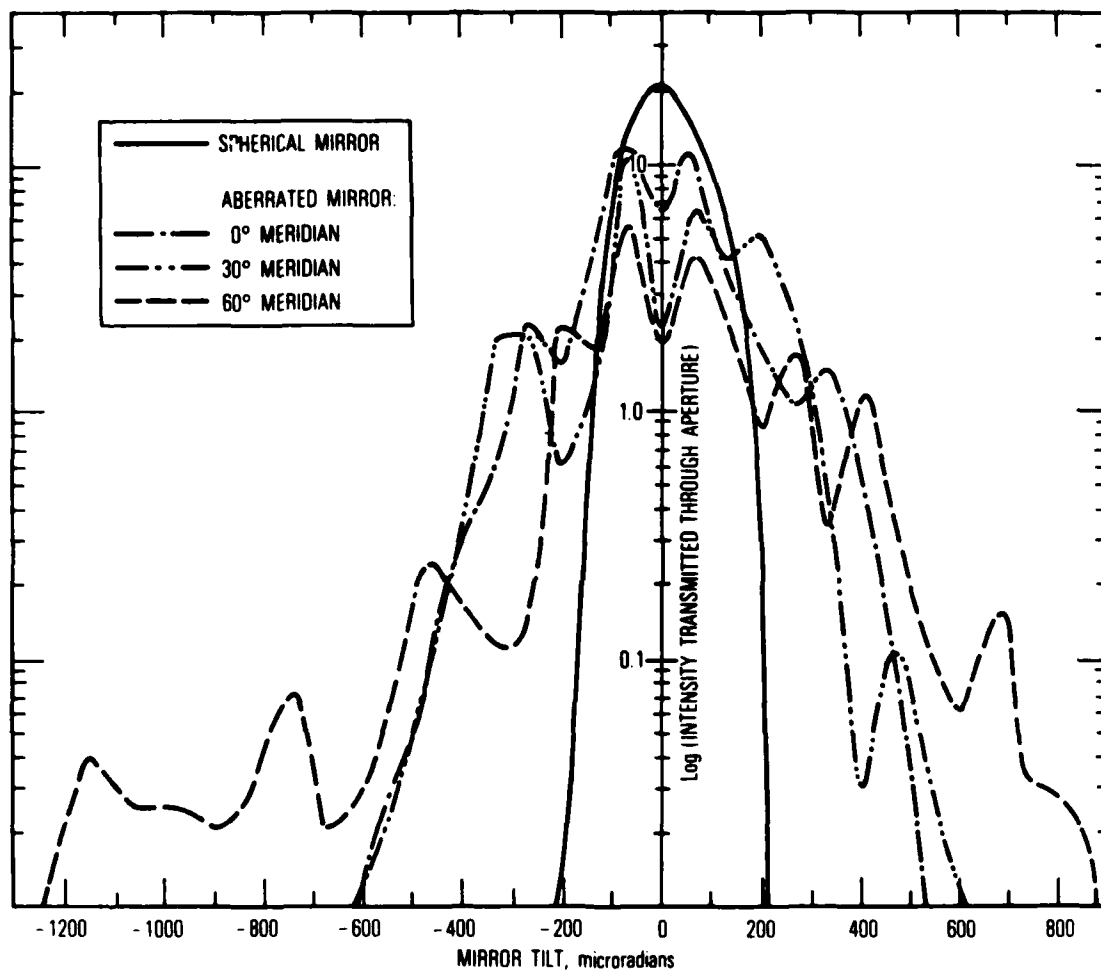
Fig. 9.   Reflectance of the Aberrated Relay Mirror as a Function of Angle, along Three Meridians 30° Apart, Compared with the Same Measurement Taken on an Optically Flat Mirror
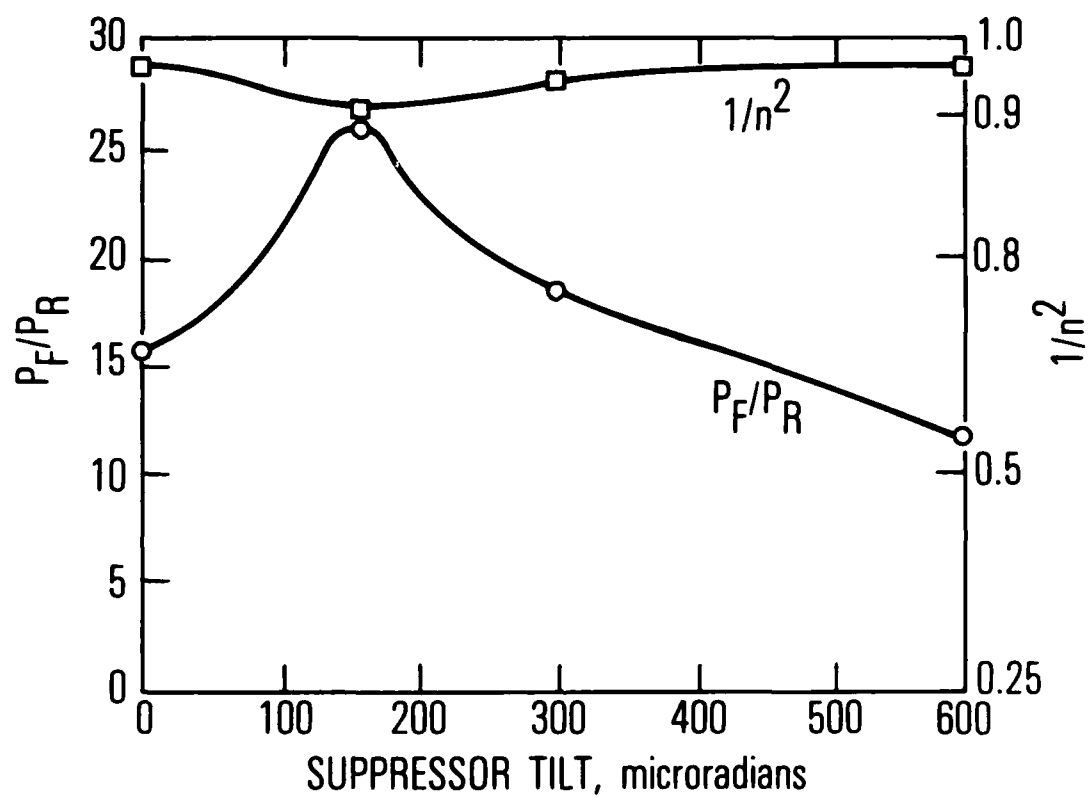
28

Fig. 10. Measured Sensitivity of Forward-to-Reverse-Wave Power Ratio and
Beam Quality to Horizontal Tilt of the Suppressor Mirror, Using
an Aberrated Relay Mirror. N_{eq} = 0.5.

IV. CONCLUSIONS

The effect of suppressor mirror reflectivity and tilt on CW HF unstable ring laser performance has been evaluated in terms of P_F/P_R, $1/n^2$, and P_F/n^2. A systematic variation of suppressor mirror reflectivity yielded results that tend to validate Eq. (1) and the theory of Ref. 6, and indicate an intrinsic backscatter reflectivity of the order $R_b^{\pm} = O(10^{-4})$ for the present resonators. A conventional reverse-wave suppressor mirror system yielded the best resonator performance, but was sensitive to suppressor mirror tilt. An aberrated relay mirror was found to provide uniform far-field brightness over a 600-μrad tilt range.

REFERENCES

1. F. R. Faxvog and A. D. Gara, "Traveling-Wave Gas Lasers," Appl. Phys. Lett. 25, 306 (1974).

2. F. R. Faxvog, "Modes of a Unidirectional Ring Laser," Opt. Lett. 5, 285 (1980).

3. R. J. Frieberg, P. P. Chenausky, and C. J. Buczek, "Unidirectional Unstable Ring Lasers," Appl. Opt. 12, 1140 (1973).

4. R. J. Frieberg, P. P. Chenausky, and C. J. Buczek, "Asymmetric Unstable Traveling-Wave Resonators," IEEE Journ. Quantum Electron. QE-10, 279 (1974).

5. Ying-Moh Liu, "Experimental Properties of an Inhomogeneously Broadened He-Xe Unstable Ring Laser," Master's Thesis, The University of New Mexico, Albuquerque, N.M. (1983).

6. H. Mirels, R. A. Chodzko, J. M. Bernard, R. R. Giedt, and J. G. Coffer, "Reverse-Wave Suppression in Unstable Ring Resonator," The Aerospace Corporation, Technical Report No. SD-TR-84-36. Also AIAA Paper #84-1649, presented at the AIAA 17th Fluid Dynamics, Plasma Dynamics, and Lasers Conference (25-27 June 1984).

7. R. A. Chodzko et al., "Zero-Power Gain Measurements in CW HF(DF) Laser by Means of Fast Scan Technique," IEEE Journ. Quantum Electron. QE-12 (11) (November 1976).

8. J. M. Bernard, D. H. Ross, J. G. Coffer, R. A. Chodzko, and S. B. Mason, "Spectrometer for Temporal Measurement of Each Output Line of Multiline HF Lasers," Appl. Opt. 23, 104-107 (1984).

9. G. Dente, W. J. Schafer Associates, Albuquerque, N.M., private communication.

10. P. Latham, AFWL, Kirtland Air Force Base, Albuquerque, N.M., private communication.

LABORATORY OPERATIONS

The Laboratory Operations of The Aerospace Corporation is conducting experimental and theoretical investigations necessary for the evaluation and application of scientific advances to new military space systems. Versatility and flexibility have been developed to a high degree by the laboratory personnel in dealing with the many problems encountered in the nation's rapidly developing space systems. Expertise in the latest scientific developments is vital to the accomplishment of tasks related to these problems. The laboratories that contribute to this research are:

Aerophysics Laboratory: Launch vehicle and reentry fluid mechanics, heat transfer and flight dynamics; chemical and electric propulsion, propellant chemistry, chemical dynamics, environmental chemistry, trace detection; spacecraft structural mechanics, contamination, thermal and structural control; high temperature thermomechanics, gas kinetics and radiation; cw and pulsed chemical and excimer laser development including chemical kinetics, spectroscopy, optical resonators, beam control, atmospheric propagation, laser effects and countermeasures.

Chemistry and Physics Laboratory: Atmospheric chemical reactions, atmospheric optics, light scattering, state-specific chemical reactions and radiative signatures of missile plumes, sensor out-of-field-of-view rejection, applied laser spectroscopy, laser chemistry, laser optoelectronics, solar cell physics, battery electrochemistry, space vacuum and radiation effects on materials, lubrication and surface phenomena, thermionic emission, photosensitive materials and infrared detectors, atomic frequency standards, and environmental chemistry.

Computer Science Laboratory: Program verification, program translation, performance-sensitive system design, distributed architectures for spaceborne computers, fault-tolerant computer systems, artificial intelligence, microelectronics applications, communication protocols, and computer security.

Electronics Research Laboratory: Microelectronics, solid-state device physics, compound semiconductors, radiation hardening; electro-optics, quantum electronics, solid-state lasers, optical propagation and communications; microwave semiconductor devices, microwave/millimeter wave measurements, diagnostics and radiometry, microwave/millimeter wave thermonic devices; atomic time and frequency standards; antennas, RF systems, electromagnetic propagation phenomena, space communication systems.

Materials Sciences Laboratory: Development of new materials: metals, alloys, ceramics, polymers and their composites, and new forms of carbon; non-destructive evaluation, component failure analysis and reliability; fracture mechanics and stress corrosion; analysis and evaluation of materials at cryogenic and elevated temperatures as well as in space and enemy-induced environments.

Space Sciences Laboratory: Magnetospheric, auroral and cosmic ray physics, wave-particle interactions, magnetospheric plasma waves; atmospheric and ionospheric physics, density and composition of the upper atmosphere, remote sensing using atmospheric radiation; solar physics, infrared astronomy, infrared signature analysis; effects of solar activity, magnetic storms and nuclear explosions on the earth's atmosphere, ionosphere and magnetosphere; effects of electromagnetic and particulate radiations on space systems; space instrumentation.

END

FILMED

3-86

DTIC